Energy Reports 9 (2023) 2269–2285

Contents lists available at ScienceDirect

Energy Reports

journal homepage: www.elsevier.com/locate/egyr

Research Paper

Multi-objective optimization of energy-saving measures and operation parameters for a newly retrofitted building in future climate conditions: A case study of an office building in Chengdu

Bo Gao [a], Xiaoyue Zhu [b], Jing Ren [c], Jingyu Ran [c], Moon Keun Kim [d], Jiying Liu [c,*]

[a] School of Mechanical Engineering, Southwest Jiaotong University, Chengdu 610030, China
[b] Sichuan Institute of Building Research, Chengdu 610084, China
[c] School of Thermal Engineering, Shandong Jianzhu University, Jinan 250101, China
[d] Department of Built Environment, Oslo Metropolitan University, Oslo 0130, Norway

A R T I C L E I N F O

Article history:
Received 19 August 2022
Received in revised form 8 October 2022
Accepted 12 January 2023
Available online xxxx

Keywords:
Multi-objective optimization
Climate change
Newly retrofitted office building
Energy savings
NSGA-II

A B S T R A C T

The energy-saving measures and suitable operation parameters will be urgent concerns in future global climate change conditions. However, a critical review revealed that most studies considered upgrading the wall insulation and glazing in the design process or the retrofit stage for existing buildings built before the twenty-first century and neglected improving system energy efficiency and operation of newly retrofitted buildings with higher-performance envelopes in the context of the carbon peak and carbon neutrality. Therefore, a real and newly retrofitted office building in Chengdu was investigated. The effect of indoor cooling and heating temperature setpoints, water supply/return temperature setpoints for the air-conditioning system, night ventilation settings in summer, and renewable energy variables (photovoltaic) are considered in the optimization. The simulation model was validated using the monitored heating and cooling energy consumption. Transient system simulation coupled with jEPlus + an evolutionary algorithm and the non-dominated sorting genetic algorithm were used to explore the optimal solution to reduce carbon emission and energy consumption while ensuring acceptable indoor thermal comfort. The sensitivity analysis showed night ventilation duration and the air change rate had significant effects on carbon emission reduction. The annual carbon emission reduction of the building was 46500–58500 kg from 2030 to 2060 using a photovoltaic panel area of 1000 m^2. The indoor temperature setpoint decreased over time due to the increasing outdoor temperature in the future. Moreover, the building energy system showed a better performance when the air source heat pump cooling setpoint was increased from 7 °C to 9 °C. Decreasing the air source heat pump heating setpoint from 45 °C to 42.5 °C for 2030 and 2060, and from 45 °C to 40 °C for 2040 and 2050 were the optimal solutions. The proposed approach provides guidance for operators to optimize energy savings and operation parameters under future climate conditions.

© 2023 The Author(s). Published by Elsevier Ltd. This is an open access article under the CC BY-NC-ND license (http://creativecommons.org/licenses/by-nc-nd/4.0/).

1. Introduction

Global climate change has been gained significant attention due to its greatest threat to humanity and global ecosystems in the coming years (Hoegh-Guldberg et al., 2019). The 5th Assessment Report (AR5) issued by the Intergovernmental Panel on Climate Change (IPCC) in 2013 indicated that relative to the average from year 1850 to 1900, global surface temperature change by the end of the 21st century is projected to likely exceed 1.5 °C (IPCC, 2013), with the maximum range of 2.6–4.8 °C based on the new representative concentration pathway (Tootkaboni et al., 2021). In this context, the building sector has received increasing attention and bore more responsibility with attempts to limit its energy consumptions and greenhouse gas emissions (Berardi and Jafarpur, 2020; Wang and Chen, 2014).

For the global building sector in 2009, the total greenhouse gas emission was 5.7 billion tons in 2009, contributing 23% of the total greenhouse gas emissions produced by the global economics activities (Huang et al., 2018). Note that numerous buildings that will exist in 2050 have already been designed and constructed (Tommerup and Svendsen, 2006); thus, the construction area is expected to increase to around 78 billion m^2 by 2050 (Güneralp et al., 2017). In China, the building sector accounted for about 40% of the total energy consumption and about 38% of national greenhouse gas emissions of economic activities. Similarly, it has been predicted that the building energy use in China will increase

* Correspondence to: School of Thermal Engineering, Shandong Jianzhu University, #1000 Fengming Road, Jinan 250101, China.
E-mail address: jxl83@sdjzu.edu.cn (J. Liu).

https://doi.org/10.1016/j.egyr.2023.01.049
2352-4847/© 2023 The Author(s). Published by Elsevier Ltd. This is an open access article under the CC BY-NC-ND license (http://creativecommons.org/licenses/by-nc-nd/4.0/).

to 1772 Mtce in 2050, which is approximately 80% higher than the current use in 2015 (Guo et al., 2021).

Therefore, it is widely recognized that improving the energy efficiency of a significant number of existing buildings is crucial to combating climate change and achieving the global carbon reduction target by 2050 (Guo and Huang, 2020). Currently, building optimization, especially multi-objective optimization, represents a rigorous methodological framework for developing energy-efficient designs (Costa-Carrapiço et al., 2020; Liu and Pouramini, 2021). Therefore, optimizing the energy-saving measures is essential to ensure the effective energy-saving design for existing buildings in future climate conditions.

1.1. Literature review on future climate conditions and impact on building energy use

The majority of energy in the building sector is used for space heating and cooling. Thus, heating, ventilation, and air-conditioning (HVAC) systems are the target for reducing energy consumption while providing acceptable occupants' thermal comfort conditions. Due to a predicted rise in cooling energy consumption under climate change and a significant contribution of the building sector to heatwaves, a growing number of studies have focused on future climate conditions and their impact on building energy consumption. This research is summarized in the following paragraphs.

In order to generate future weather data files, the morphing method (Belcher et al., 2005) has been used to generate future weather data files due to its simplicity and flexibility (Wang and Chen, 2014). It combines a baseline hourly weather data file with future monthly weather variables predicted by a global climate model (Chai et al., 2019; Zou et al., 2021b; Wang and Chen, 2014). Several studies chose this method and conducted dynamic energy simulations to predict future weather conditions and determine the effect of climate change on building energy consumption (Olonscheck et al., 2011; Tootkaboni et al., 2021).

Shen (2017) used the morphing method to downscale and obtain local hourly weather data to predict the annual energy use of representative residential and office buildings in the USA. The results indicated that energy use was predicted to increase from −1.64% to 14.07% and −3.27% to −0.12% during 2040–2069, respectively, due to climate change.

Berardi and Jafarpur (2020) used statistical downscaling to create future weather files to assess the heating and cooling demand of 16 buildings in Canada. The results showed an average decrease of 18%–33% and an average increase of 15%–126% for heating energy use and cooling energy use by 2070, respectively.

Several studies have focused on the effect of climate change on building energy use in Chinese climatic zones (Li et al., 2020; Meng et al., 2018; Wan et al., 2012). The changes in building energy use for heating and cooling in representative cities with different future climates were estimated for Harbin (Chai et al., 2019), Kunming (Wang et al., 2021b), Chengdu (Nurlybekova et al., 2021), Hong Kong (Wan et al., 2011), Guangzhou (Zou et al., 2021b), with target years from 2050 to 2100. The results indicated a shift in the electricity demand due to an increase in cooling energy. A significant decrease in heating energy use occurred, e.g., decreases of 14.2, 7.2, and 7.1 W/m^2 in Harbin, Tianjin, and Shanghai, respectively, in cold and extremely cold climate zones where the heating energy dominates (Li et al., 2020; Meng et al., 2018). Therefore, the impact of future climate change on building energy use demonstrates the importance of considering climate change in the design and retrofitting of buildings in Chinese climate zones.

1.2. Literature review on energy-saving measures in future climate conditions

The above studies demonstrate the significance of considering future climate conditions/scenarios to evaluate building energy use and implement mitigation measures at the building and urban scale (Azimi Fereidani et al., 2021). Due to differences in the scale of the studies and urban morphologies (Javanroodi et al., 2018), the building density, building type, canopy geometry, building height-to-street width ratio, and building compactness were not reviewed. Most studies focused on decreasing the heat gain and reducing energy use at the building scale and classified the strategies into passive and active measures (Azimi Fereidani et al., 2021; Hu et al., 2021). The most common passive strategies included the use of thermal insulation (Karimpour et al., 2015), highly reflective materials (Vasaturo et al., 2018), shading (D'Agostino et al., 2022), efficient glazing (Oree et al., 2016), green roofs (Andric et al., 2020), improved building airtightness (Wang et al., 2021b), and cooling ventilation (Jimenez-Bescos, 2017). Active measures comprised renewable energy systems (Jalilzadehazhari et al., 2021), including rooftop photovoltaic (PV) systems (Ascione et al., 2021; Chai et al., 2019), adjustment of the temperature setpoints (Bienvenido-Huertas, 2021; Jafarpur and Berardi, 2021), and energy-efficient operation strategies of the HVAC system (He et al., 2021).

Designing appropriate thermal insulation and thermal mass could be an efficient measure to cope with global warming, while shading devices can reduce carbon emissions and are insensitive to global warming (Radhi, 2009). It was also found that a smaller window-to-wall ratio reduced the negative effect of climate change on energy use (Berardi and Jafarpur, 2020). Efficient glazing can reduce energy consumption for heating and cooling by up to 50% (Sarihi et al., 2021). In addition, the addition of green walls and roofs can mitigate the effect of climate change and heat islands compared to the usage of energy-efficient windows (Andric et al., 2020). Therefore, different measures should be further considered in different climate zones to identify the positive or negative effects of the insulation levels.

Furthermore, night ventilation (NV) may be an effective adaptive measure to reduce the cooling requirements and greenhouse gas emissions of buildings under climate change, although its performance is highly dependent on climate conditions (Gilani and O'Brien, 2021). NV, including natural and/or mechanical ventilation with passive operation strategies and optimization measures, is effective in most climate zones (Solgi et al., 2018), e.g., in many Southern and Central European buildings (Artmann et al., 2008). A case study of London Islington under different future climate and emission scenarios revealed that NV with an air change rate (ACH) of 10 h^{-1} reduced overheating by less than 8% for medium emissions scenarios (Jimenez-Bescos, 2017). Meanwhile, a mixed ventilation mode, which maximized the use of natural ventilation during favorable outdoor conditions and mechanical cooling systems when natural ventilation was insufficient, significantly reduced energy use in office buildings in Australia (Bamdad et al., 2022). Therefore, it is essential to consider the suitability of different ventilation strategies and the buildings' lifespan under climate change.

Moreover, changing the thermostat setpoints is an effective method for saving energy under future climate conditions (Bienvenido-Huertas, 2021; Hoyt et al., 2015). Adjusting the temperature setpoints reduced the annual energy demand by 0.9–8.7% in Quebec City, 1.6–9.1% in Toronto, and 1.4–9.9% in Vancouver (Jafarpur and Berardi, 2021). It was also found that increasing the indoor setpoint cooling temperature from the current 18 °C to 22 °C in Qatar resulted in significant annual energy savings of up to 30%. The improvement was equivalent to retrofitting the building with expanded polystyrene but without the additional investment (Andric et al., 2020). However, obtaining considerable energy savings depends on the climate zone, building type, and the desired level of thermal comfort (Bienvenido-Huertas et al., 2020).

Installing PV systems with an energy storage system in new or existing buildings is an option for electricity production and can be highly efficient under climate change (Azimi Fereidani et al., 2021). Due to the advances in PV technologies and more supporting policies, PV systems are expected to be widely implemented in China in the 21st century (Zhao et al., 2020). In addition to PV systems, other renewable energy sources (biomass, wind, and geothermal systems) and efficient HVAC systems and equipment should be adopted after cost optimization (D'Agostino and Parker, 2018).

The literature review showed that existing and effective mitigation measures are highly dependent on future climate conditions, the building envelope characteristics, operation strategies, efficient technologies, and the occupants' behavior. Indeed, a majority of the reviewed studies considered upgrading the wall insulation and glazing of existing buildings built before 2010 during the design or retrofit stage. However, this approach overestimates energy consumption and energy savings and ignores the impact of climate change on existing highly insulated buildings that are currently built (e.g., after 2015). A review of studies on efficient adaptation and mitigation measures under climate change indicates a lack of studies on operation and energy-saving measures for newly built or newly retrofitted buildings under future climate conditions. Due to an increase in the urbanization level, nearly zero-energy buildings will be constructed widely based on the newest national standards. Therefore, the impacts of future climate change scenarios, e.g., in 2050, on the energy implications of operation and energy-saving measures for newly-built or newly-retrofitted buildings have to be investigated.

1.3. Literature review on multi-objective optimization of energy-saving measures and operation parameters considering climate change

Different optimization methods need to be considered to achieve a trade-off solution, e.g., between energy consumption, thermal comfort, and building cost due to the local climate and global warming impacts (Lapisa et al., 2018). Building performance optimization is an effective and widely used method to provide a rigorous framework for optimizing energy-efficient measures and operation strategies under climate change (Ameur et al., 2020; Harkouss et al., 2018). Based on the number of objective functions, optimization algorithms have been classified into single-objective and multi-objective methods. Multi-objective optimization can be used to explore passive and active measures to optimize building energy consumption (Wang et al., 2021a), daylighting (Bamdad et al., 2021), life cycle cost (Xue et al., 2022), discomfort hours (Ascione et al., 2019), and ventilation potential (Grygierek and Ferdyn-Grygierek, 2018).

Recently, multi-objective optimization studies have explored operation measures and retrofit strategies to address the impact of different climate conditions on buildings (Shao et al., 2014). However, the vast majority of optimization studies have focused on energy consumption optimization of existing buildings under different climate scenarios (Chang et al., 2020; Costa-Carrapiço et al., 2020). Few studies focused on the design of energy-optimized buildings to assess the energy, environmental, and economic impacts using the present climate-optimized building in the future climate (D'Agostino et al., 2022; Sobhani et al., 2020). The popular approach is coupling the multi-objective optimization method and a building energy simulation to conduct numerous calculations, and finally obtain a trade-off solution for the operation parameters and objective functions (Zou et al., 2021a).

The literate review indicated that the non-dominated sorting genetic algorithm II (NSGA-II) has been widely used due to its efficient computation, better solutions, and strong ability to consider population diversity using the crowding distance (Ghaderian and Veysi, 2021; Vukadinović et al., 2021). The most frequently considered optimization variables were related to the building envelope (U-value, insulation thickness, and shading) (Zou et al., 2021a), glazing characteristics (Bamdad et al., 2021), building orientation (Ansah et al., 2022), and infiltration (Nguyen et al., 2021). Furthermore, the staged optimization was limited to the building parameters (shape, orientation, thermal physical properties); however, renewable energy use, system operation variables, and control methods were not comprehensively considered in the context of climate change.

1.4. Summary of literature review and research scope

The literature review revealed that climate change and its impact on building energy use have been extensively investigated in representative cities and mainland China. The vast majority of studies have focused on energy-saving measures in future climate conditions. Most studies used multi-objective optimization to determine passive and active measures for optimizing building energy consumption, thermal comfort, and other objective functions. It should be noted that most reviewed studies considered upgrading the wall insulation and glazing in the design process or the retrofit stage for existing buildings built before the twenty-first century. However, some newly-built buildings, e.g., nearly zero-energy buildings, will become more widespread in the context of carbon peak and carbon neutrality. Therefore, more studies are required to quantify the effects of future climate change on performance of the newly-built buildings taking into account the operation strategies and suitability of renewable energy system.

Accordingly, this study conducts a multi-objective optimization of energy-saving measures and operation parameters for a newly-retrofitted office building in future climate conditions and analyzes the influence of the operation variables on carbon emissions and thermal discomfort hours (TDH). A newly retrofitted office building in 2018 in Chengdu city with a three-star green rating is selected as the research target. Future weather data are firstly generated for 2030, 2040, 2050, and 2060 using the morphing method based on the weather data of a typical meteorological year (TMY) in Chengdu city, China. Different indoor cooling and heating temperature setpoints, water supply/return temperature setpoints of the HVAC system, night ventilation settings in summer, and renewable energy variables (PV) are selected to investigate the sensitivity of the future-climate optimized operation to different parameters. The proposed approach provides guidance for operators to optimize energy savings, maintain acceptable indoor thermal comfort, and obtain the operation parameters under future climate conditions.

2. Methodology

2.1. Research framework

Fig. 1 illustrates the modeling and multi-optimization workflow using transient system simulation (TRNSYS) and jEPlus + EA. In this figure, the two dotted red boxes represented the modeling stage and multi-objective optimization stage with the adopted two tools, respectively. First, a building model was established in the TRNSYS for multi-objective optimization according to the building characteristics, including the physical and geometric

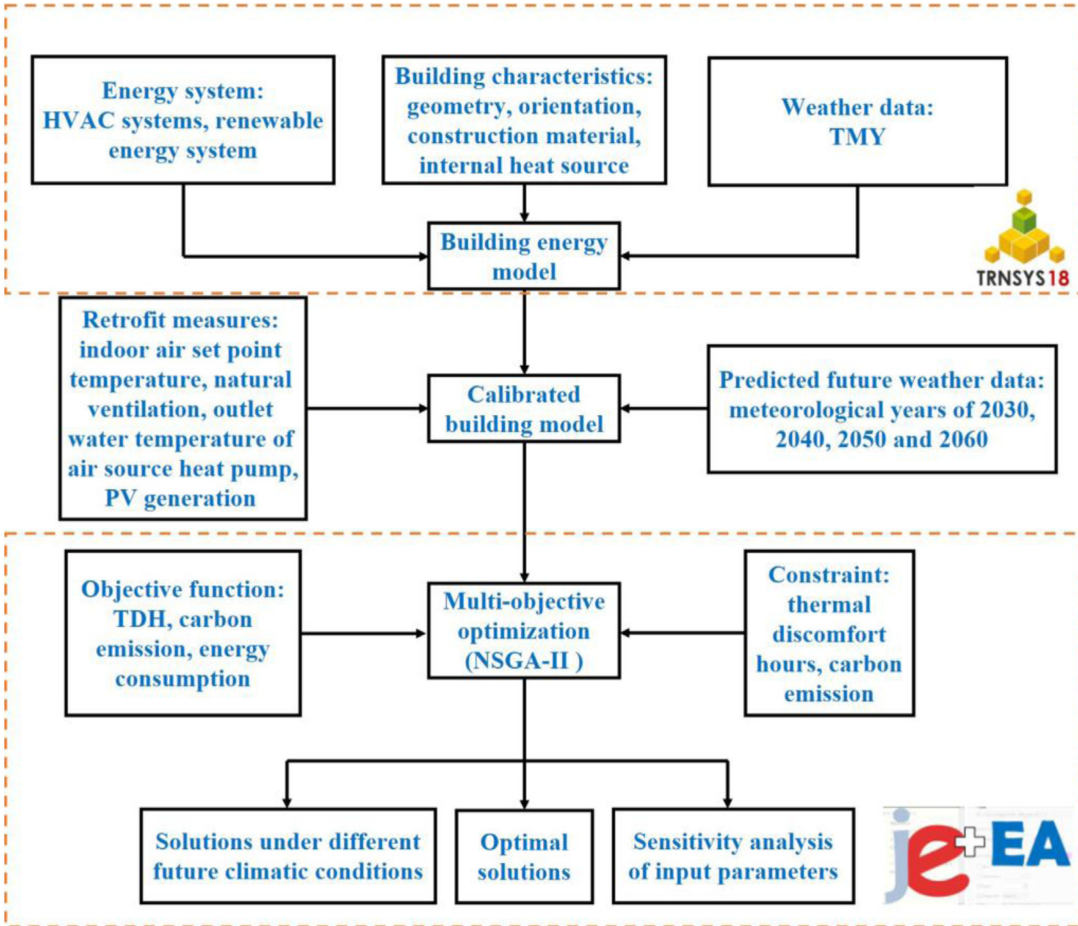

Fig. 1. The research framework of this study.

parameters and the internal heat source (Klein et al., 2006). The building model was equipped with an HVAC system and a renewable energy system. The established building energy model with the input weather data of a TMY was calibrated.

Then the operation measures were applied to the building model, including the indoor air setpoint temperature, NV, outlet water temperature of the air source heat pump, and PV generation. The four predicted weather data files for the meteorological years of 2030, 2040, 2050, and 2060 were used in the optimization process. Multi-objective optimization was conducted using jEPlus + EA with the NSGA-II algorithm including different objection functions and constraints to obtain the optimal solutions.

Moreover, the solutions for different future climatic conditions were compared to determine suitable operation measures in response to a warming climate. Meanwhile, sensitivity analysis was carried out to evaluate the influence of the operation variables on the optimal solutions.

2.2. Building description

The newly retrofitted building is located in Chengdu city in southwestern China. Chengdu city is located in a mild climate region with hot summers and cold winters; there are four distinct seasons, abundant rainfall, and moderate sunshine hours. The office building has an area of about 150 000 m^2. There are 13 floors with a height of 4.5 m for the first floor and 3.7 m for the other floors.

Fig. 2 shows photos of the building before and after the retrofit. The building was constructed in 1989 and retrofitted in 2017. Comprehensive reinforcement, environmental improvement, and energy efficiency improvement resulted in better insulation and energy-efficient performance of the building. The annual energy consumption per area was reduced from 38.44 kWh/m^2 to 36.19 kWh/m^2. Table 1 shows the building construction materials and the overall heat transfer coefficients (U-value).

The retrofitted building was equipped with PV for energy generation to reduce carbon emissions. The HVAC system is a fan coil unit with an outdoor air supply. The configurations of the equipment are shown in Fig. 3. The air source heat pump (ASHP) serves as a cold and heat source for the air conditioning system; it has a coefficient of performance (COP) with an annual average of 3.35. The design supply and return water temperature is 7/12 °C in summer and 45/40 °C in winter. NV during summer nights is employed to cool down the indoor air and building envelope. The grid-connected PV system covers an area of 182.52 m^2 with a capacity of 10 kW. Table 2 presents the design conditions of the internal heat gains and outdoor air rate for building performance simulation.

2.3. Climate change prediction method

The AR5 of the IPCC was published in 2013 and proposed several new scenarios and climatic models to represent the physical and chemical processes of the planet's climate system (Church et al., 2013). Total radiative forcing (RF_{tot}) was used to describe and quantify climate change, e.g., the value is 2.29 Wm^{-2} due to an increase in CO_2 concentration in the atmosphere from 1975 to 2011. The representative concentration pathway (RCP) is based on the approximate calculation of the RF_{tot} in the year 2100

Fig. 2. Photos of the building before (a) and after (b) the retrofit.

Table 1
Construction materials for retrofitting the building and comparison of the overall heat transfer coefficients.

Building components	Layer materials (newly retrofitted)	U-value (W/m^2 K)	
		Newly retrofitted	Pre-retrofit
Exterior wall	2 cm Cement mortar 24 cm Aerated concrete block 2 cm Cement mortar	0.99	2.45
Roof	4 cm Fine aggregate concrete 2 cm Cement mortar protective layer 4 cm Extruded polystyrene board 0.4 cm Asphalt waterproof coiled material 2 cm Cement mortar leveling course 3 cm Cement expanded perlite 2 cm Cement mortar leveling course 12 cm Reinforced concrete roof slab 2 cm Cement mortar	0.65	2.13
Floorslab	2 cm Cement mortar 10 cm Reinforced concrete 2 cm Cement mortar	0.98	3.89
Window	6 mm medium light transmittance Low-E 6+9A+6+9A+6	2.4	6.5

Fig. 3. The schematic diagrams of the PV and HVAC systems. (a) fan coil, (b) outdoor air system for night mechanical ventilation, and (c) PV.

relative to the year 1750 (Verichev et al., 2020). There are four scenarios: RCP2.6 (van Vuuren et al., 2011), RCP4.5 (Thomson et al., 2011), RCP6.0 (Masui et al., 2011), and RCP8.5 (Riahi et al., 2011). Those four scenarios indicate different conditions of global socio-economic development and different levels of greenhouse emissions. The RCP4.5 represents a stable scenario with $RF_{tot} = 4.5$ Wm^{-2} in 2100, a peak in the population of 9 billion inhabitants in 2065, and 8.7 billion in 2100 (Verichev et al., 2020). Thus,

Table 2
Design conditions of internal heat gains and outdoor air flow rate.

Parameters	Design value
Occupancy	0.067 person/m^2
People load	66 W/person
Equipment load	15 W/m^2
Lighting load	9 W/m^2
Outdoor air flow rate	30 m^3/h

Table 3
NMBE and CVRSME for different HVAC components.

	HVAC terminal		Water pump and ASHP	
	Cooling	Heating	Cooling	Heating
NMBE	3.83%	2.45%	2.29%	3.56%
CVRSME	15.14%	12.96%	11.59%	8.29%

this scenario was selected to investigate the potential effects of climatic change in the current climate zone of Chengdu city on building energy consumption (Zhai and Helman, 2019).

Global climate models use monthly weather data, whereas the simulation of building energy consumption requires hourly weather data, e.g., TMY data. Morphing method is a widely used downscaling method, which combines the existing meteorological parameter time series with climate change through shift and stretch to generate a new meteorological parameter file while retaining the physical characteristics of the existing meteorological parameters (Belcher et al., 2005). Therefore, the morphing method was used to downscale the predicted monthly weather data to hourly data (e.g., outdoor air temperature, solar radiation). Three morphing methods were used, including shift, stretch, and a combination of shift and stretch methods (Guan, 2009).

(1) Shift method

$$x = x_0 + \Delta x_m \tag{1}$$

where x represents the future hourly weather variables, x_0 denotes the original hourly climatic variables, Δx_m is the absolute change in the monthly mean value of the variables for month m.

(2) Stretch method

$$x = \alpha_m x_0 \tag{2}$$

where a_m is the fractional change in the monthly mean value for month m (Zou et al., 2021a).

(3) Combination of shift and stretch method

$$x = x_0 + \Delta x_m + \alpha_m \times (x_0 - \langle x_0 \rangle_m) \tag{3}$$

where $\langle x_0 \rangle_m$ is the monthly average value of the climatic variable x_0 for month m.

The combined method was used for the dry bulb temperature to generate data for 8760 h in a year. The scaling factor α_{mt} for the dry bulb temperature was calculated as follows:

$$\alpha_{mt} = \frac{\Delta T_{max,m} - \Delta T_{min,m}}{t_{max,m} - t_{min,m}} \tag{4}$$

where $\Delta \mathrm{T}_{max,m} - \Delta \mathrm{T}_{min,m}$ is the average monthly temperature change predicted by the RCP4.5 climate model, $t_{max,m} - t_{min,m}$ is the average monthly temperature change of the current weather file.

The meteorological dataset of the Chinese standard weather data (CSWD) is jointly developed by the China Meteorological Administration and Tsinghua University. It is based on measured weather data from ground weather stations in China. The CSWD are hourly data of TMYs used in the simulation of building energy consumption (Energyplus, 2022). Consequently, this study used the TMY weather data and generated future weather data using the morphing method for 2030, 2040, 2050, and 2060.

2.4. Building energy system model

2.4.1. Simulation and optimization tool

This study used TRNSYS to conduct the building performance simulation. This software is a powerful simulation tool with a flexible modular structure and includes building geometry data and location information. It is suitable for renewable energy simulations with different operation strategies (Liu et al., 2019; Ren et al., 2022). Energy-saving measures were adopted, including PV and NV. A renewable energy system (PV) was used to generate energy for the building. NV was used as a passive energy technology (Guo et al., 2020) to supplement cooling when the cooling system was shut down. The PV panels were modeled using module Type 94a. The control functions related to the NV control were defined in the module equations. The ASHP (module Type 941), water pump (module Type 110), and fan coil (module Type 928) comprised the air-conditioning system. The system operation depended on schedule controllers (module Type 41 and 14) and temperature controllers (module Type 2). The established TRNSYS model for the building energy system is shown in Fig. 4.

Based on the study background and purpose, building optimization design was used to evaluate the different techniques and obtain optimal results. jEPlus + EA is a multi-objective optimization algorithm suitable for building optimizations. It has a user-friendly environment and a graphical interface and can import data from TRNSYS (Naji et al., 2021). Thus, jEPlus + EA coupled with TRNSYS was used for conducting the multi-objective optimization. The optimization process is shown in Fig. 5.

2.4.2. Building energy model calibration

This study utilized the normalized mean bias error (NMBE) and the coefficient of variation of the root mean squared error (CVRMSE) to evaluate the accuracy of the simulation model (ASHRAE, 2002). They are defined in Eqs. (5) and (6).

$$\mathrm{NMBE} = \frac{\sum_{i=1}^{n} (y_i - \check{y}_i)}{(n - \mathrm{p}) \times \bar{\mathrm{y}}} \times 100\% \tag{5}$$

$$\mathrm{CVRMSE} = \frac{\left[\sum_{i=1}^{n} (y_i - \check{y}_i)^2 / (n - p)\right]^{1/2}}{\bar{\mathrm{y}}} \times 100\% \tag{6}$$

where $\check{y}_i$ denotes the predicted data, y_i is the calibrated data, and $\bar{\mathrm{y}}$ is the average value with p = 1. Note that the NMBE should be lower than 5%, and the CVRMSE should be lower than 15%, according to the ASHRAE guideline 14-2014.

Fig. 6 presents the comparison of the measured and simulated energy consumption of different HVAC components. The general variation of the heating and cooling energy consumption was captured by the simulation. Table 3 lists the calculated NMBE and CVRSME for different HVAC components. Note that the cooling and heating consumption CVRSME for the HVAC terminal were 15.14% and 12.96%, respectively, only slightly larger than the 15% threshold. The NMBEs of the cooling and heating consumption of the ASHP and water pump were 11.59% and 8.29%, respectively. The NMBEs for different HVAC components were lower than the 5% threshold and satisfied the standard requirements.

The error was acceptable since real-time solar data and accurate indoor occupant behavior were used for the simulation. Therefore, the comparison indicates that the model meets the requirements.

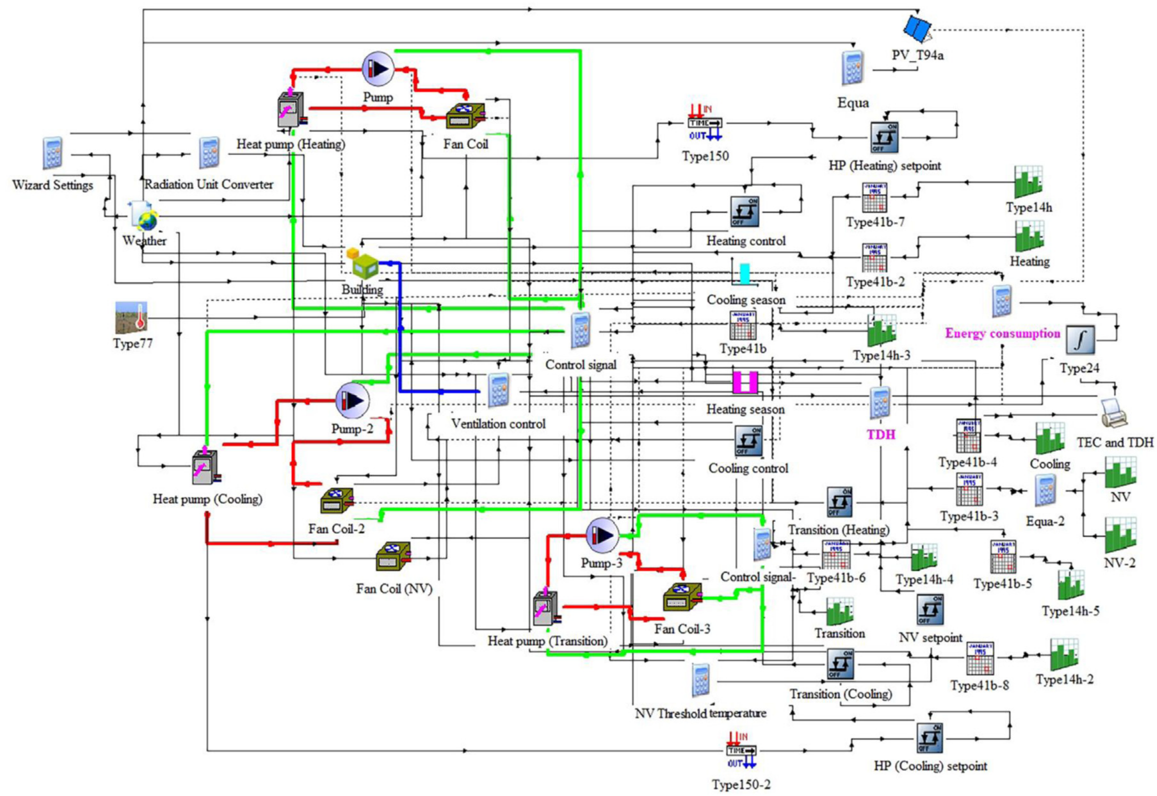

Fig. 4. TRNSYS model of the building energy system.

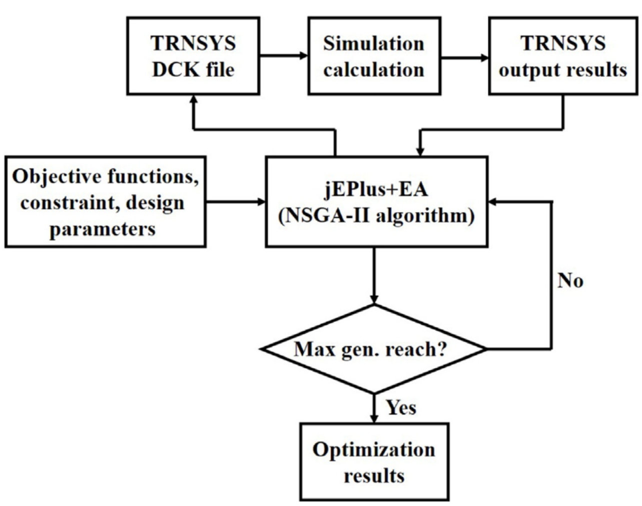

Fig. 5. Optimization process using TRNSYS and jEPlus + EA.

2.5. Multi-objective optimization problem design

2.5.1. Mathematical description

Three objectives are considered in the multi-objective optimization problem: building energy consumption, carbon emissions, and indoor thermal comfort. The objective functions and constraints constitute the multi-objective optimization problem. The mathematical description of the multi-objective optimization is as follows (Bingham et al., 2019):

Minimize:

$$F\left(\vec{x}\right) = [f_1\left(\vec{x}\right), f_2\left(\vec{x}\right), \ldots f_k\left(\vec{x}\right)]^T \tag{7}$$

Subject to:

$$\vec{g}(\vec{x}) \le 0 \;\; and \;\; \vec{h}(\vec{x}) = 0 \tag{8}$$

where:

$$\vec{x} \in R^n,\;\; \vec{f}\left(\vec{x}\right) \in R^k,\;\; \vec{f}\left(\vec{x}\right) \in R^m \;\; and \;\; \vec{h}(\vec{x}) \in R^q \tag{9}$$

$$X = \{\vec{x}\,|g_m(\vec{x}) \le 0, m = 1, 2, 3\cdots m\} \tag{10}$$

$$\{h_q\left(\vec{x}\right) = 0, q = 1, 2, 3\cdots q\} \tag{11}$$

$$S = \{F(\vec{x})|\vec{x} \in X\} \tag{12}$$

where $\vec{x} \in R^n$ is the vector of the operation variables, k is the number of objective functions; it is set to 3 in this study; m is the number of inequality constraints, n is the number of decision variables, $\vec{f}\left(\vec{x}\right) \in R^k$ is an objective vector where $\vec{f_i}\left(\vec{x}\right) : R^n \rightarrow R^1$, $\vec{g}(\vec{x})$ is the vector of the inequality constraints, q is the number of equality constraints, $\vec{h}(\vec{x})$ is the vector of equality constraints, X is the feasible decision, and S is the criterion space (Delgarm et al., 2016).

2.5.2. Optimization objective functions and optimization constraints

Three optimization objectives were considered, including indoor thermal comfort, energy consumption, and carbon emissions. The TDH were used to indicate the level of discomfort.

(1) TDH

$$f_1(x) = \min\left(\int 1dt \;for\; |PMV| > 0.5 + \int 0dt \;for\; |PMV| \le 0.5\right) \tag{13}$$

where t is the simulation timestep, h; PMV is the predicted mean vote, which is calculated according to the ASHRAE 55-2013 standard (ASHRAE, 2013).

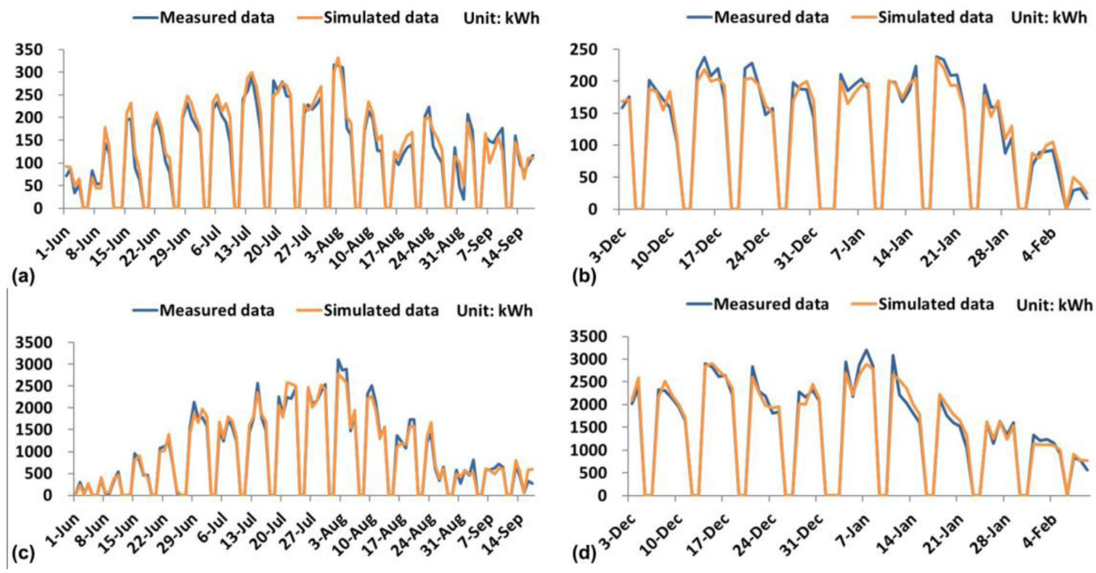

Fig. 6. Comparison of daily energy consumption for different HVAC components, (a) HVAC terminals in summer, (b) HVAC terminals in winter, (c) ASHP and water pump in summer, (d) ASHP and water pump in winter.

(2) Carbon emissions

$$TEC = E_{HP} + E_{pump} + E_{fan} = \frac{Q}{COP} + \frac{\rho_w g H V_w}{1000\eta_{pump}} + \frac{\Delta P \times V_a}{\eta_{fan}} \quad (14)$$

$$f_2\,(x) = \min[1.15\ (TEC - PVE)] \quad (15)$$

where E_{HP} is the energy consumption of the heat pump, kWh; E_{pump} is the energy consumption of the water pump, kWh; E_{fan} is the energy consumption of the fan, kWh; Q is the cooling capacity of the heat pump, kWh; COP is the coefficient of performance; ρ_w is the density of water, kg/m^3; H is the pump head, m; V_w is the water flow rate, m^3/h; η_{pump} is the water pump efficiency; ΔP is the pressure rise through the fan, Pa; V_a is the air flow rate, m^3/s; η_{fan} is the fan efficiency; TEC is the total energy consumption of the building energy system, kWh; PVE is the electricity generated by the PV system, kWh. The electricity not used by the building energy system was sent to the utility power grid for energy savings. A coefficient of 1.15 for total energy consumption was selected according to the Chinese life cycle database (Xue et al., 2022).

The optimization problem has two constraints. First, the maximum allowable TDH were 789 h (García Kerdan et al., 2017), which was the design level when the building energy system was in the rated operation without optimized measures. Second, the carbon emissions of the building energy system were limited to less than 41.4 kg per area per year (MOHURD, 2021).

2.5.3. Renewable energy system and optimization operation variables

Cooling and heating setpoints are essential for determining carbon emissions. A higher cooling setpoint and lower heating setpoint minimize the energy consumption and reduce carbon emissions. In addition, choosing suitable on/off temperature setpoints for the ASHP in winter and summer results in energy savings and improvements in indoor thermal comfort conditions. The literature review indicated that NV should be considered. The NV flow rate or ACH setpoint, activation threshold temperature, minimum indoor temperature setpoint, and ventilation duration are crucial operation variables. The PV panel area and PV tilt influence the PV performance. It is feasible and common to consider these two variables in the optimization process.

Therefore, we chose commonly used variables included in the TRNSYS module. Table 4 presents the building optimization operation parameters. The abbreviations P1-P10 were used to represent the HVAC system setpoints, PV variables, NV setting in summer variables, and the ASHP setpoints, respectively.

2.6. Optimization method

2.6.1. NSGA-II method

The NSGA-II is a multi-objective genetic algorithm based on the fast non-dominated sorting genetic algorithm (NSGA) (Deb et al., 2002). It has better performance and efficiency than the NSGA algorithm and is considered an effective algorithm for multi-objective optimization (Evins, 2013). This study implemented the NSGA-II algorithm in the jEPlus + EA tool.

The NSGA-II utilizes fast non-dominated sorting, the crowding degree, the crowding degree comparison operator, and an elite strategy. The time complexity of each Pareto classification in the NSGA is O(MN^3) (where M represents the target number, and N represents the population size). In contrast, the time complexity of the NSGA-II is O(MN^2); thus, it has a higher sorting speed. The elite strategy refers to passing on excellent individuals in the parent population to the offspring population to create the next-generation population and preserve the genetic potential of excellent individuals. The crowding degree and crowding degree comparison operator are used to replace the shared parameters that need to be manually specified to ensure population diversity. The calculation formula of the crowding distance of the i_{th} solution is as follows:

$$i_d = \sum_{k=1}^{m} \frac{f_k\,(i+1) - f_k(i-1)}{f_k^{max} - f_k^{min}}, 2 \le i \le n-1 \quad (16)$$

where i_d is the crowding distance, $f_k\,(i+1)$ denotes the $(i+1)_{\text{th}}$ objective function values, $f_k(i-1)$ denotes the (i-1)$_{\text{th}}$ objective function values, f_k^{max} and f_k^{min} are the maximum and minimum values of the objective function, respectively. NSGA-II is used to solve the multi-objective optimization problem in conjunction with TRNSYS (Xie et al., 2020). Fig. 7 presents the flowchart of the NSGA-II method using the jEPlus + EA tool.

2.6.2. Optimization parameters setting

The multi-objective optimization used the NSGA-II algorithm to improve the adaptive fit of the candidate populations using

Table 4
Building optimization operation parameters.

Categories	Parameters		Variable types	Range/values	Units
HVAC system indoor setpoints	P1	Cooling setpoint	Discrete	24, 25, 26, 27	°C
	P2	Heating setpoint	Discrete	17, 18, 19, 20	°C
PV variables	P3	PV panel area	Discrete	400, 600, 800, 1000	m^2
	P4	PV tilt	Discrete	10, 15, 20, 25	°
Variables for the summer NV	P5	Night ACH setpoint	Discrete	1 to 5, interval 0.4	h^{-1}
	P6	Activation threshold temperature	Discrete	1 to 3, interval 0.2	°C
	P7	Minimum indoor temperature setpoint	Discrete	20 to 24, interval 0.4	°C
	P8	Ventilation duration	Discrete	18:00–21:00, 18:00–22:00, 18:00–23:00, 18:00–24:00	h
ASHP setpoints	P9	On/off temperature setpoint in winter	Discrete	(37.5, 32.5), (40, 35), (42.5, 37.5), (45, 40)	°C
	P10	On/off temperature setpoint in summer	Discrete	(7, 12), (8, 13), (9, 14), (10, 15)	°C

**: on/off setpoint indicates the return water setpoint for ASHP system.

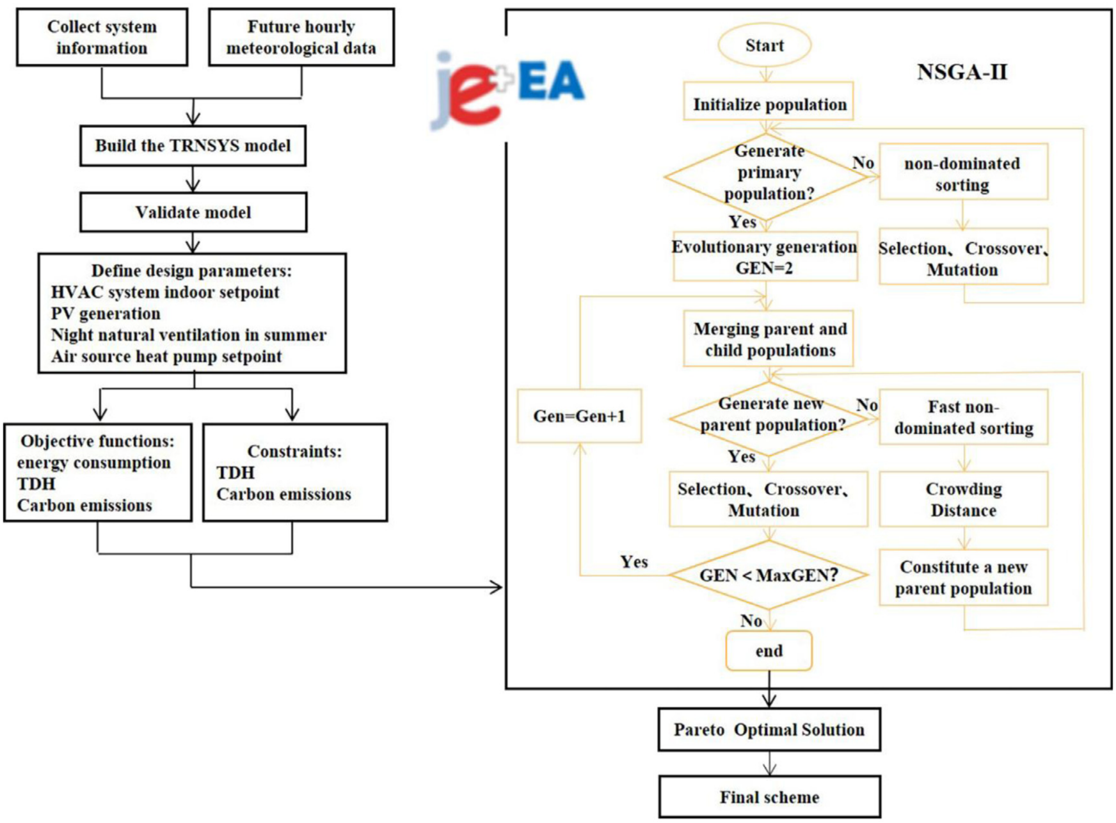

Fig. 7. Flowchart of the NSGA-II method.

non-dominated sorting and Pareto dominance. The population reproduces and evolves to produce individuals more suitable for obtaining the optimal solution. The population size was 25, parallel simulations were conducted, and the maximum number of generations was 200. The crossover probability and mutation probability were 90% and 20%, respectively, resulting in a compromise between the computational complexity and accuracy. The total computer execution time was approximately 120 h. Table 5 summarizes the NSGA-II initialization parameters.

Table 5
The parameters for NSGA-II initialization.

Parameters	Value
Population size	25
Crossover	0.9
Mutation	0.2
Tournament selector	2
Maximum generations	200
Total simulations	5000

3. Results

3.1. Sensitivity analysis of operation variables

Fig. 8 illustrates the influence of the ten operation variables on carbon emissions and TDH in 2050. The results were the same in the other three years. The input and the output parameters are positively (negatively) correlated when the standard coefficient is positive (negatively). A larger absolute value of the standard coefficient indicates that the variable has a larger influence on the output parameters. In the linear regression model of carbon emissions (Fig. 8a), P1, P2, P9, and P10 were the most influential factors affecting carbon emissions. The carbon emissions generally increased as P1 and P10 decreased. In contrast, reducing P2 and P9 caused a decrease in carbon emissions. The optimization of the operation variables related to night NV resulted in a greater reduction in carbon emissions.

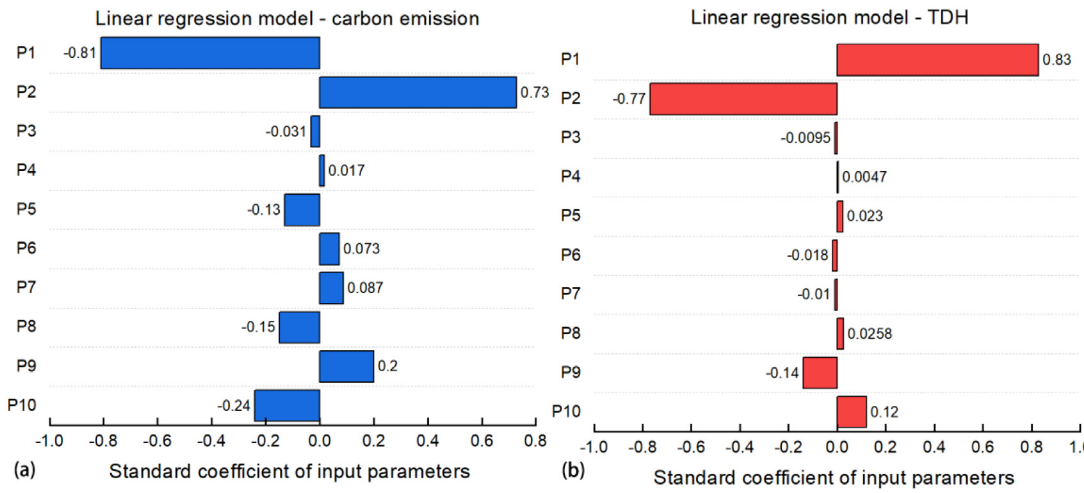

Fig. 8. Standard coefficient of operation variables for the linear regression model of (a) carbon emissions and (b) TDH.

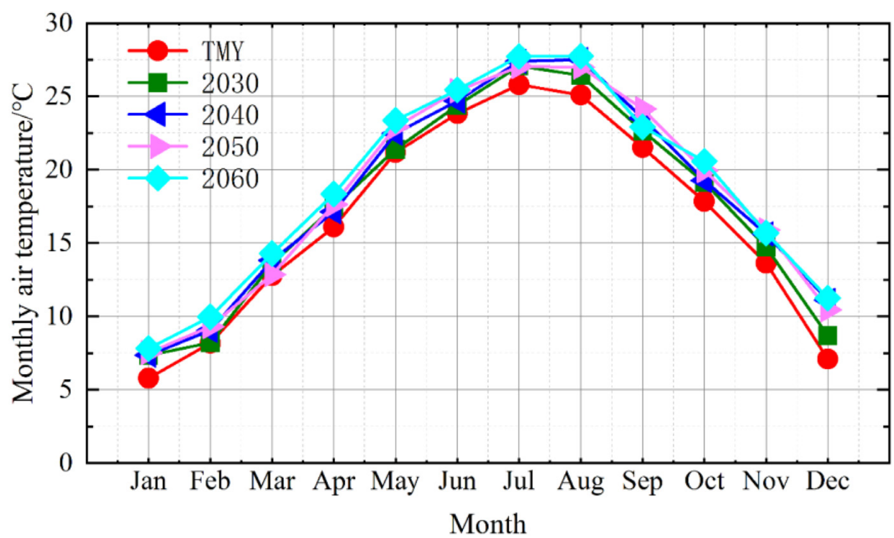

Fig. 9. Monthly average temperature for the TMY, 2020, 2040, 2050, and 2060.

In the linear regression model of TDH (Fig. 8b), P1 was the most influential parameter, followed by P2, P9, and P10. NV with larger P8 and P5 values reduced the TDH while decreasing P6 increased the TDH. This result indicates that increasing NV cooling and setting a higher NV requirement results in more efficient cooling and a more comfortable indoor thermal environment. Besides, a higher P7 prevented overcooling by NV and decreased the TDH. In addition, using more night cooling decreased the TDH. These findings indicate that more night cooling should be adopted to reduce the energy consumption of the ASHP and prevent overcooling.

3.2. Solutions for different future climatic conditions

We first present the results for the future weather data. Fig. 9 shows the monthly average temperature for the TMY, 2020, 2040, 2050, and 2060. The largest temperature increases occurred in November and December, and the smallest occurred in February, March, and June. Fig. 10 summarizes the annual average air temperature in Chengdu city. The yearly average dry bulb temperature is about 1.0 °C higher in 2030, 1.7 °C higher in 2040, 1.8 °C higher in 2050, and 2.2 °C higher in 2050 than in the TMY.

Fig. 11 showed simulated TDH and carbon emission under different meteorological year conditions in the future. The results integrates the solutions obtained by the optimization method under different meteorological year conditions in the future. The solutions showed similar trends as the Pareto distribution. At least one objective was improved without adversely affecting the other objectives. The difference in the solutions for different years was due to the warmer climate from 2030 to 2060. For the multi-objective minimization with constraints, the carbon emission showed an increasing tendency, and the TDH slightly increased as the external temperature increased from 2030 to 2060. In addition, the number of infeasible solutions increased year after year because the thermal comfort level could not be reached, or the upper limit of carbon emissions was exceeded. Therefore, it is necessary to retrofit existing buildings to improve energy efficiency due to increasing difficulties in maintaining a satisfactory thermal comfort level in the future.

3.3. Operation variable distribution

Since the variations in the carbon emissions and TDH were more significant in 2050, we focused on the operation variable before and after optimization in 2050 (Fig. 12). Fig. 12a and b present the operation variable distributions of the solutions for carbon emissions and TDH, respectively. In the plots, each column

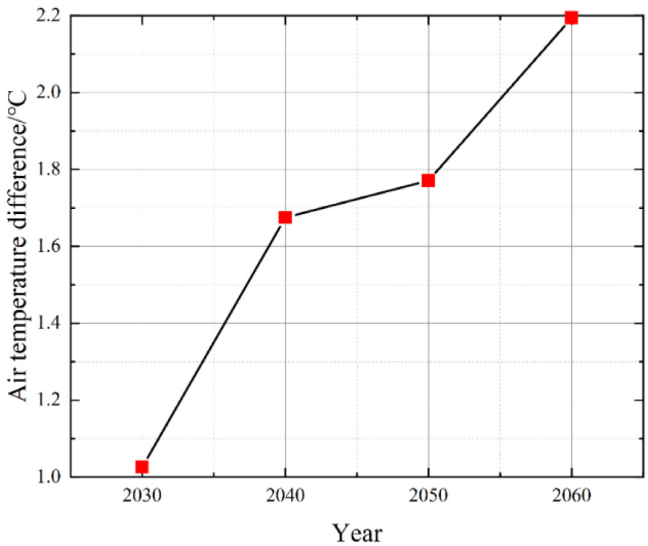

Fig. 10. Annual average air temperature difference in Chengdu city compared to the TMY.

represents one input parameter, and ten operation variables were optimized in this simulation. The values of the different operation variables of a solution in the columns are connected by a line. The variable distribution related to the optimal solutions obtained from the optimization algorithm and range of objectives are shown in Fig. 12c and d.

More colors were clustered in the columns corresponding to P1, P2, P9, and P10, reflecting the main effect of the indoor temperature setpoint and the ASHP setpoint on the optimization result. Moreover, P1, P2, P7, and P8 have a smaller range, and a single value was obtained for P3 and P4 in the optimal solutions, resulting in a simplified optimization process. A smaller search space results in better optimization performance. Meanwhile, P5, P6, P9 and P10 values showed higher variability, indicating that NV depended more on P7 and P8; thus, the optimization process was more targeted, providing better supplementary cooling performance. The range of carbon emissions and TDH were 36.5∼40.5 kg/m^2 and 300∼600 h after the optimization. The values of the carbon emissions were close to the upper limit, whereas the TDH had lower values, revealing that reducing carbon emissions was more challenging in the optimization.

3.4. Effect of NV duration on carbon emissions

Fig. 13 shows the effect of the NV duration and night ACH setpoint on carbon emissions under different future climatic conditions. Each point represents the average value of carbon emissions of the Pareto optimal solutions with a specific NV duration or night ACH setpoint for a concise comparison. The NV duration had a significant effect on carbon emissions. As shown in Fig. 13a, When the NV duration was extended from 3 h (18:00∼21:00) to 6 h (18:00∼24:00), the carbon emissions decreased in all future climatic conditions. The reduction in carbon emissions ranged from 0.8% to 5% for the 2030 to 2060 scenarios. This result indicated that extending the NV duration could contribute to a decrease in future carbon emissions.

The night ACH setpoint was also an influential factor affecting carbon emissions. A higher ACH setpoint improved the cooling efficiency by countering heavy indoor loads. However, Fig. 13b shows a smaller reduction in carbon emission caused by an increase in the ACH setpoint compared with the effect of the NV duration. It is unreasonable to solely use a high ACH setpoint because night cooling requires sufficient cooling energy without the need for a high indoor cooling rate. It is necessary to prevent overcooling and an instable cooling supply caused by an ACH setpoint with a high start–stop frequency. Therefore, more than 5 h NV duration and a lower ACH setpoint should be used to ensure a stable operation and sufficient cooling while minimizing carbon emissions.

3.5. Optimal combination of PV panel parameters

The PV panel area and tilt are crucial parameters affecting the PV performance for electricity production. A highly efficient PV

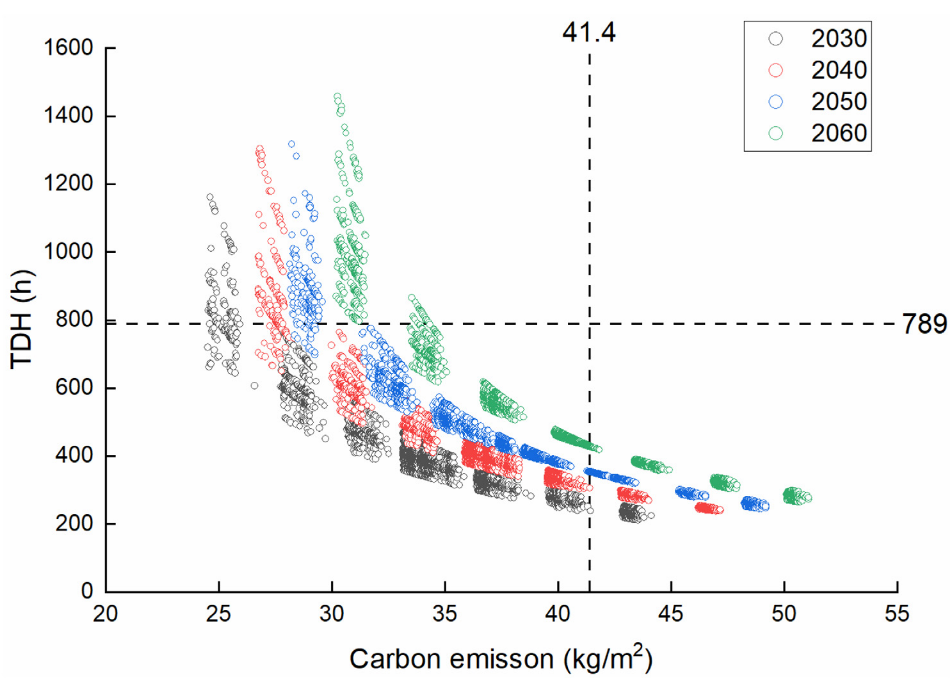

Fig. 11. The simulated TDH and carbon emission in 2030 to 2060.

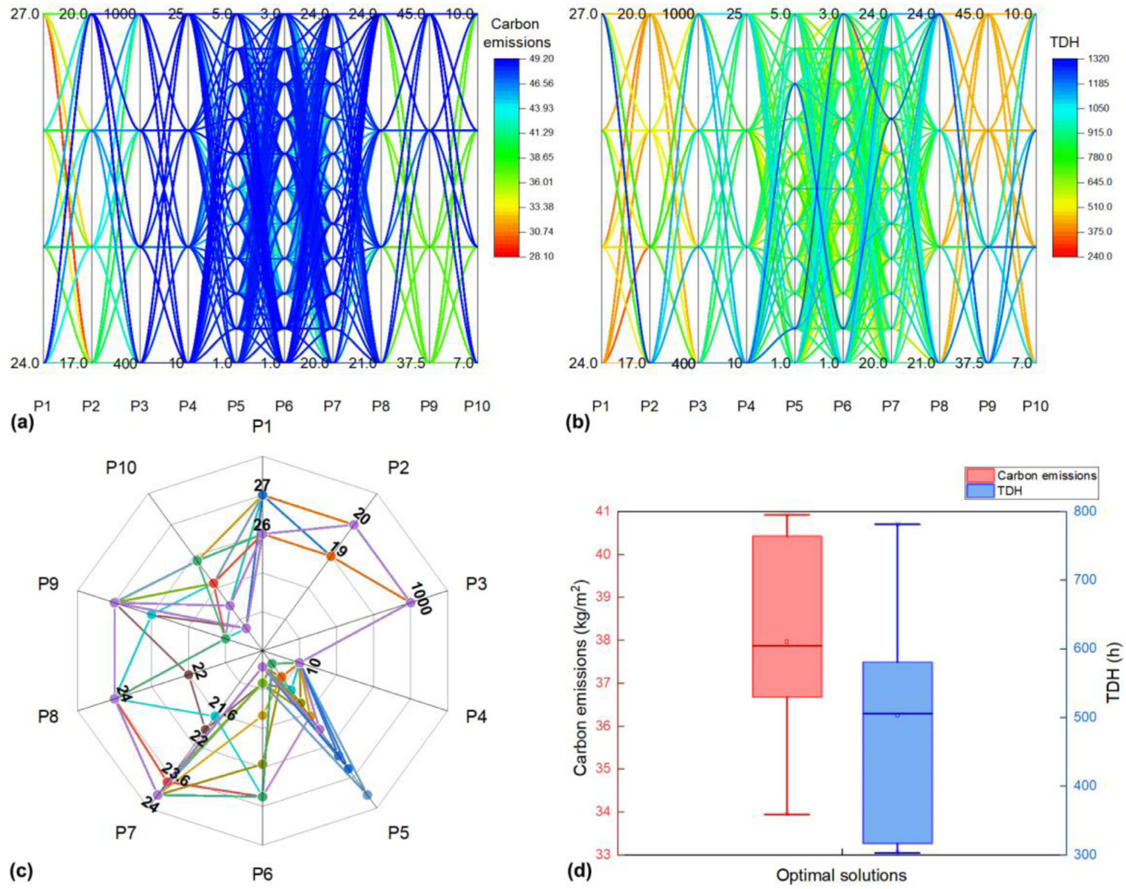

Fig. 12. Operation variable distributions. (a) total variable distribution related to carbon emissions, (b) total variable distribution related to TDH, (c) optimal variable distribution, and (d) range of carbon emissions and TDH.

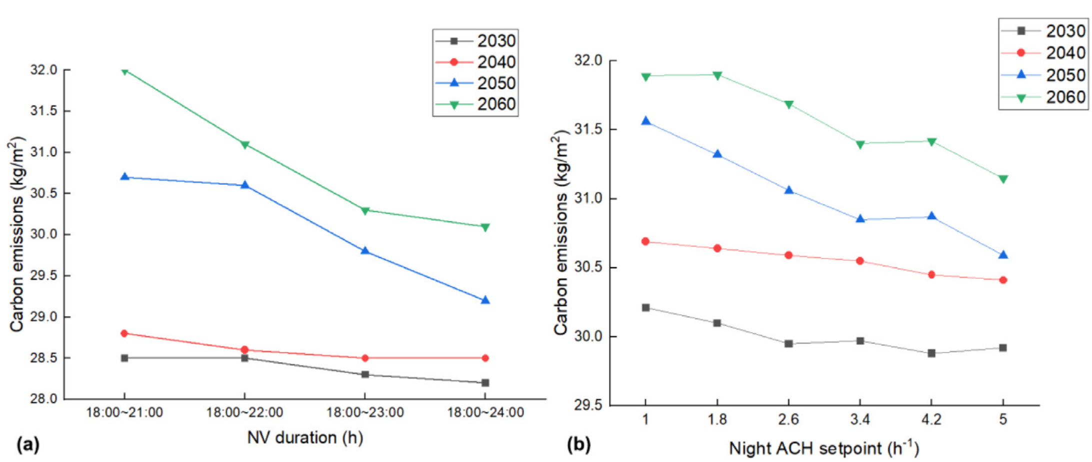

Fig. 13. Carbon emissions for different (a) NV durations and (b) night ACH setpoints.

system is critical for providing supplementary electricity. Fig. 14 shows the effect of different combinations of PV panel parameters on carbon emissions. The colored surface shows the average carbon emissions obtained from the Pareto optimal solutions for a specific PV panel area and PV tilt. A change in the PV tilt resulted in a greater change in carbon emissions than a change in the PV panel area. The carbon emissions increased with an increase in the PV tilt, while the effect of the PV panel area on carbon emissions was unclear.

A decrease in the PV tilt in the range of 10–25° resulted in a notable decrease in carbon emissions due to greater absorption of direct solar radiation. The maximum decreases in carbon emissions for the 2030 to 2060 scenarios were 0.39 kg/m^2, 0.31 kg/m^2, 0.33 kg/m^2, and 0.34 kg/m^2, respectively. The equivalent decrease for the whole building was 46 500–58 500 kg/a, showing significant potential for carbon emission reduction. Meanwhile, the correlation between the PV panel area and carbon emissions was inconsistent. In addition, a large PV panel area and a smaller tilt resulted in the lowest carbon emission in the four climatic conditions, indicating the potential for high power generation and a reduction in carbon emissions.

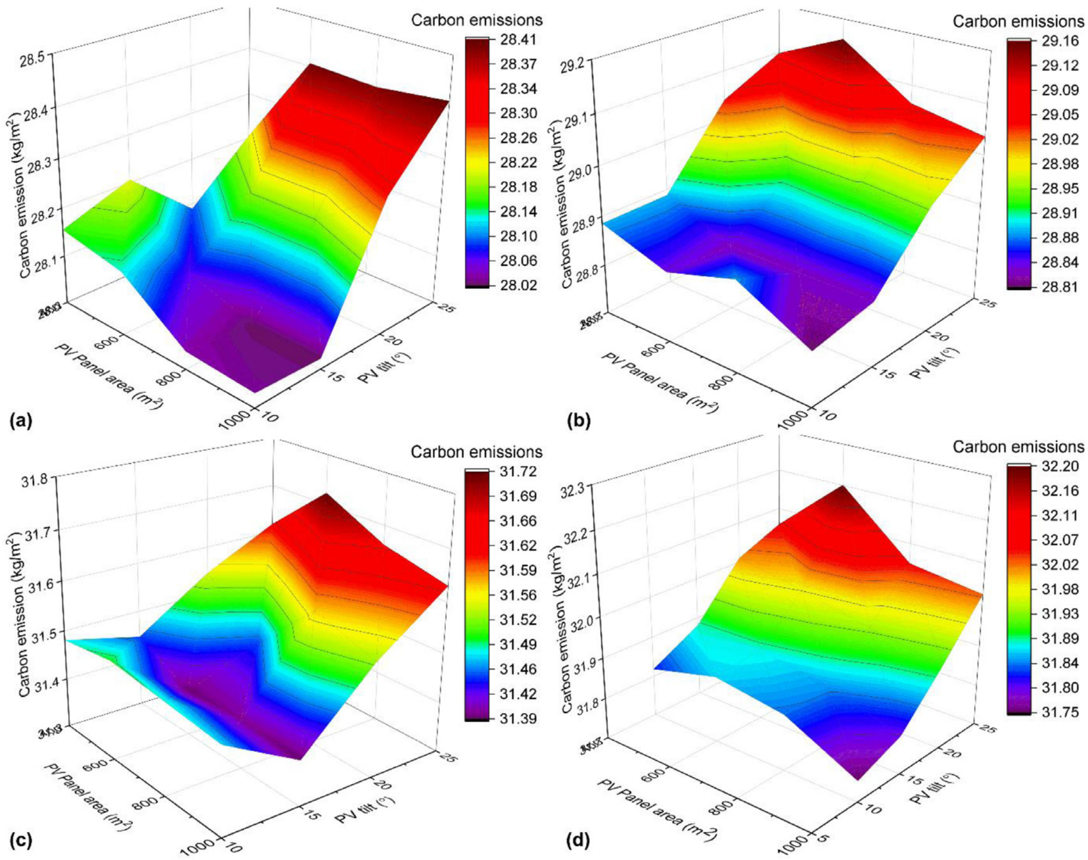

Fig. 14. Effect of different PV panel areas and tilts on carbon emissions in (a) 2030, (b) 2040, (c) 2050, and (d) 2060.

3.6. Effect of cooling and heating setpoints

A common control method of HVAC systems is the selection of different cooling and heating setpoints to establish ON/OFF criteria. The indoor temperature level remains relatively stable for different cooling/heating setpoints. Therefore, using an appropriate indoor temperature setpoint provides a suitable thermal environment while preventing unnecessary energy waste.

Fig. 15 shows the feasible solutions for different cooling and heating setpoints. The lowest cooling and heating setpoints were eliminated due to high energy consumption and unsatisfactory TDH constraints. A cooling setpoint of 26 °C accounted for approximately half of the total feasible solutions. Setpoints lower than 25 °C and 26 °C showed increasingly significant advantages in the 2030 to 2060 scenarios. Most of the feasible solutions had a heating setpoint of 20 °C. The proportion of solutions with a heating setpoint of 18 °C was significantly higher in 2060 than in the other years. The results indicated that the increasingly warmer climate in the future affected the cooling and heating setpoints. Thus, when the cooling/heating requirement could not be met, the cooling/heating setpoint should be adjusted to improve indoor thermal comfort while minimally increasing carbon emissions. When the building energy system has low efficiency, the cooling/heating setpoint must be optimized to reduce carbon emissions while minimizing an increase in TDH.

3.7. Effect of adjusting the on–off temperature setpoint of the ASHP

The ASHP provides cooling/heating energy for air conditioning. The outlet water temperature is a critical parameter in determining the cooling/heating capacity of the ASHP. Higher temperature supply water from the ASHP for heating improves indoor thermal comfort but causes more carbon emissions, and lower temperature water for cooling has the same effect within a reasonable temperature range.

Figs. 16a and 6b shows the average value of carbon emissions and TDH of the feasible solutions when the temperature setpoint is decreased by 2.5 °C and increased by 1 °C in winter and summer. Decreasing (increasing) the temperature setpoint from 45 °C to 42.5 °C (from 7 °C to 8 °C) caused the largest relative increase in carbon emissions and TDH, respectively.

The variation gradient corresponding to an increase in TDH for every 1 kg/m^2 decrease in carbon emissions when the temperature setpoint is increased (decreased) by 1 °C (2.5 °C) in summer (winter) is listed in Fig. 16 to evaluate the effect of changing the temperature setpoint. A decrease in the heating setpoint from 45 °C to 42.5 °C (42.5 °C to 40 °C) for 2030 and 2060 (for 2040 and 2050) resulted in a minimum variation gradient. When the cooling setpoint was increased from 8 °C to 9 °C for the four years, the variation gradient was minimum. An appropriate setpoint temperature provides significantly better thermal comfort with a relatively small increase in carbon emissions.

4. Discussion

This study figured out the optimal solutions related to energy-saving measures and operation parameters for a newly retrofitted building using TRNSYS and jEPlus + EA. Both carbon emissions and energy consumption have been significantly reduced while the satisfactory indoor thermal comfort was achieved.

Due to potential problems related to thermal comfort and energy consumption caused by global warming and the shortage of non-renewable resources in the future, the energy performance of HVAC systems and installed renewable energy systems requires improvement. Therefore, this study focused on retrofitted

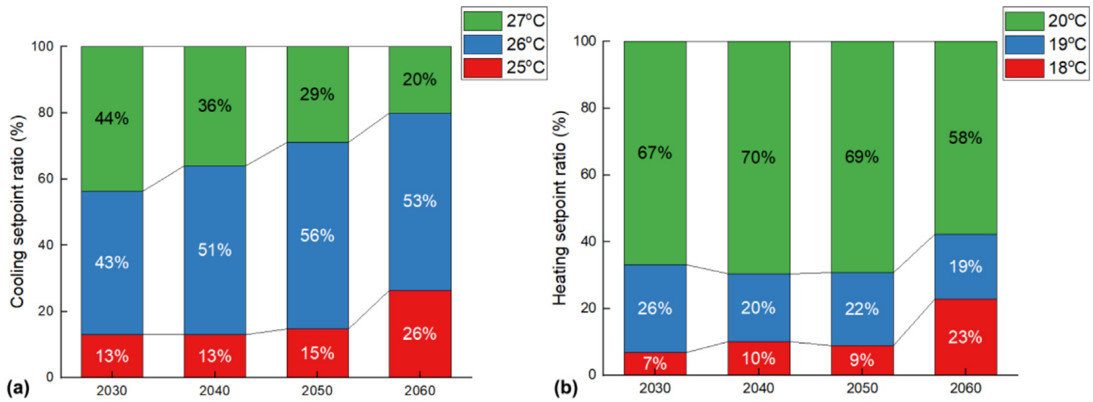

Fig. 15. The solutions with different (a) cooling setpoints and (b) heating setpoints.

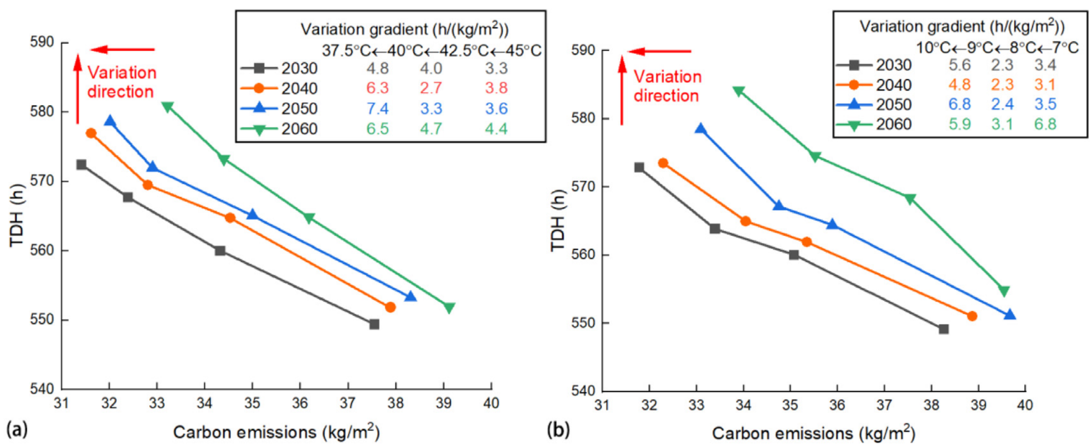

Fig. 16. The effect of adjusting the on–off temperature setpoint of the air source heat pump on carbon emissions and thermal comfort in (a) winter and (b) summer.

operation measures for an office building under future climate conditions. The night NV variables and PV variables were optimized to reduce carbon emissions. The indoor setpoint and air source heat pump setpoint were adjustable to adapt to global warming. The optimization extended the use of renewable energy technology and passive strategies and enhanced the cooling system performance to achieve acceptable thermal comfort levels and energy savings under future climate conditions.

The aim of this study was to maximize the effect of energy-saving measures and optimize the operation parameters to enhance the energy efficiency of the building energy system and meet the comfort requirements under future climate conditions. Predicted weather data for 2030, 2040, 2050, and 2060 were used in the optimization. The optimization results were also extracted from the simulation data. The effectiveness and reliability cannot be sufficiently proved without practical application. Therefore, it is necessary to improve model accuracy through modifying simulation parameters based on actual building characteristic, schedule and energy system operation and comparing building energy model with experimental data for effective optimization. Four factors related to the HVAC system were optimized including night ventilation in summer, PV parameters, HVAC system indoor setpoints, and on/off control of the ASHP. The sufficient parameter values were chosen to correspond to practical conditions of building energy systems to ensure the accuracy of the results.

The night ventilation was highly dependent on the climate condition derived from the weather data files. The influence of night ventilation cooling on carbon emission reduction may differ from actual conditions. Moreover, the dynamic change in the indoor environment affected the night ventilation performance. Therefore, operation measures for building systems should be changed according to the indoor and outdoor conditions in practical applications. For example, in this case study of an office building in Chengdu, the optimal performance of the ASHP was achieved when the cooling setpoint increased from 7 °C to 9 °C for the four years, and heating setpoint decreased from 45 °C to 42.5 °C (45 °C to 40 °C) for 2030 and 2060 (2040 and 2050).

A PV system was used to provide energy for the building energy system, and the PV panel area and panel tilt were considered in the optimization of the PV operation parameters. The excess electricity generated by PV was sent to the utility power grid to eliminate the need for batteries. Battery storage coupled with the PV system will be considered in a future study to match the building load in the simulation. More parameters of the PV-battery system can be optimized to improve renewable technology. The optimization results are reliable for practical applications. It is necessary to consider the investment cost in the objective functions and constraints to provide a cost-effective strategy.

Moreover, building energy system modeling is critical in the optimization process. The model accuracy and computational efficiency should be considered to achieve high optimization efficiency and provide a reliable optimized design. Previous studies have shown that the mutation fraction generally ranges from 0.05 to 0.4 (Costa-Carrapiço et al., 2020). The value of the mutation parameter should be kept low (10%–20%) to prevent the search process from becoming a primitive random search (Chaturvedi et al., 2020). Therefore, in the future study, we will reduce the mutation rate and conduct sufficient optimization runs to obtain more accurate results.

Finally, this study only focused on one building in Chengdu city and optimized the specified operation strategies. The office building was suitable for this experimental study on building science and developing green building technology. The building performance was improved by upgrading the wall insulation before this study. Therefore, we focused on optimizing specific operation strategies. Applying the study results to practical cases is required. Future studies will consider energy-saving measures for a generic retrofitted office building, e.g., more detailed HVAC operation parameters, comprehensive energy generation and storage systems, and complex renewable energy utilization.

5. Conclusion

This study integrated TRNSYS with jEPlus + EA to conduct multi-objective optimization of energy-saving measures and operation parameters for a newly retrofitted office building in future climate conditions. The energy performance of the HVAC systems and installed renewable energy systems was improved to face potential problems related to thermal comfort and energy consumption caused by global warming and the shortage of non-renewable resources in the future. A case study of an office building in Chengdu city was conducted.

The sensitivity analysis results demonstrated that the cooling and heating setpoint and the on/off temperature setpoint were the most influential parameters of the ASHP. The night ventilation cooling level should be increased to provide supplementary cooling and reduce the energy use of the ASHP.

Since the similar temperature conditions in the four years caused comparable effects on indoor environment, the building energy system used the same operation strategies. Extending the NV duration resulted in a reduction in carbon emissions from 0.8% to 5% from 2030 to 2060. More than 5 h NV duration and a lower ACH setpoint should be used to ensure a stable operation and sufficient cooling while minimizing carbon emissions. PV panels with a larger area and smaller tilt were required to save energy. The annual carbon emission reduction of the entire building was 46 500–58 500 kg from 2030 to 2060. The cooling and heating setpoints of the HVAC system should be increased to deal with a warming climate in the future. The optimal performance of the ASHP was achieved when the cooling setpoint increased from 7 °C to 9 °C for the four years, and heating setpoint decreased from 45 °C to 42.5 °C (45 °C to 40 °C) for 2030 and 2060 (2040 and 2050).

In future studies, we plan to combine multi-objective optimization with the advanced control of the building energy system in complex buildings in different climate zones. Moreover, it is critical to establish an integrated criterion encompassing thermal comfort, carbon emissions, energy consumption, and life cycle costs to evaluate the energy efficiency and control performance of building energy systems. Accordingly, cost-efficient control techniques will be achieved to minimize energy consumption while meeting the indoor thermal comfort requirements.

CRediT authorship contribution statement

Bo Gao: Conceptualization, Investigation, Methodology, Software, Writing – original draft, Project administration, Funding acquisition. **Xiaoyue Zhu:** Validation, Writing – review & editing. **Jing Ren:** Supervision, Investigation, Software, Writing – original draft, Writing – review & editing. **Jingyu Ran:** Investigation, Software. **Moon Keun Kim:** Methodology, Software, Writing – review & editing. **Jiying Liu:** Conceptualization, Supervision, Resources, Writing – review & editing, Project administration, Funding acquisition.

Declaration of competing interest

The authors declare that they have no known competing financial interests or personal relationships that could have appeared to influence the work reported in this paper.

Data availability

Data will be made available on request.

Acknowledgments

The work was supported by the Scientific and Technological Innovation Projects of Sichuan Provincial Department of Housing and Urban-Rural, China (SCJSKJ2021-05) and Natural Science Foundation of Shandong Province, China (ZR2021ME199, ZR2021ME237). This work was also supported by the Plan of Introduction and Cultivation for Young Innovative Talents in Colleges and Universities of Shandong Province, China.

References

Ameur, M., Kharbouch, Y., Mimet, A., 2020. Optimization of passive design features for a naturally ventilated residential building according to the bioclimatic architecture concept and considering the northern Morocco climate. Build. Simul. 13, 677–689. http://dx.doi.org/10.1007/s12273-019-0593-6.

Andric, I., Kamal, A., Al-Ghamdi, S.G., 2020. Efficiency of green roofs and green walls as climate change mitigation measures in extremely hot and dry climate: Case study of Qatar. Energy Rep. 6, 2476–2489. http://dx.doi.org/10.1016/j.egyr.2020.09.006.

Ansah, M.K., Chen, X., Yang, H., 2022. A holistic environmental and economic design optimization of low carbon buildings considering climate change and confounding factors. Sci. Total Environ. 821, 153442. http://dx.doi.org/10.1016/j.scitotenv.2022.153442.

Artmann, N., Gyalistras, D., Manz, H., Heiselberg, P., 2008. Impact of climate warming on passive night cooling potential. Build. Res. Inf. 36, 111–128. http://dx.doi.org/10.1080/09613210701621919.

Ascione, F., Bianco, N., Maria Mauro, G., Napolitano, D.F., 2019. Building envelope design: Multi-objective optimization to minimize energy consumption, global cost and thermal discomfort. Application to different Italian climatic zones. Energy 174, 359–374. http://dx.doi.org/10.1016/j.energy.2019.02.182.

Ascione, F., Bianco, N., Mauro, G.M., Napolitano, D.F., 2021. Effects of global warming on energy retrofit planning of neighborhoods under stochastic human behavior. Energy Build. 250, 111306. http://dx.doi.org/10.1016/j.enbuild.2021.111306.

ASHRAE, 2002. ASHRAE Guideline 14-2002: Measurement of Energy and Demand Savings. American Society of Heating, Refrigerating and Air Conditioning Engineers Inc., Altanta, GA.

ASHRAE, 2013. ASHRAE 55-2013: Thermal Environmental Conditions for Human Occupancy. ASHRAE, Atlanta.

Azimi Fereidani, N., Rodrigues, E., Gaspar, A.R., 2021. A review of the energy implications of passive building design and active measures under climate change in the Middle East. J. Clean. Prod. 305, 127152. http://dx.doi.org/10.1016/j.jclepro.2021.127152.

Bamdad, K., Cholette, M.E., Omrani, S., Bell, J., 2021. Future energy-optimised buildings — Addressing the impact of climate change on buildings. Energy Build. 231, 110610. http://dx.doi.org/10.1016/j.enbuild.2020.110610.

Bamdad, K., Matour, S., Izadyar, N., Omrani, S., 2022. Impact of climate change on energy saving potentials of natural ventilation and ceiling fans in mixed-mode buildings. Build. Environ. 209, 108662. http://dx.doi.org/10.1016/j.buildenv.2021.108662.

Belcher, S., Hacker, J., Powell, D., 2005. Constructing design weather data for future climates. Build. Serv. Eng. Res. Technol. 26, 49–61. http://dx.doi.org/10.1191/0143624405bt112oa.

Berardi, U., Jafarpur, P., 2020. Assessing the impact of climate change on building heating and cooling energy demand in Canada. Renew. Sustain. Energy Rev. 121, 109681. http://dx.doi.org/10.1016/j.rser.2019.109681.

Bienvenido-Huertas, D., 2021. Influence of the type of thermostat on the energy saving obtained with adaptive setpoint temperatures: Analysis in the current and future scenario. Energy Build. 244, 111024. http://dx.doi.org/10.1016/j.enbuild.2021.111024.

Bienvenido-Huertas, D., Sánchez-García, D., Rubio-Bellido, C., 2020. Comparison of energy conservation measures considering adaptive thermal comfort and climate change in existing Mediterranean dwellings. Energy 190, 116448. http://dx.doi.org/10.1016/j.energy.2019.116448.

Bingham, R.D., Agelin-Chaab, M., Rosen, M.A., 2019. Whole building optimization of a residential home with PV and battery storage in The Bahamas. Renew. Energy 132, 1088–1103. http://dx.doi.org/10.1016/j.renene.2018.08.034.

Chai, J., Huang, P., Sun, Y., 2019. Investigations of climate change impacts on net-zero energy building lifecycle performance in typical Chinese climate regions. Energy 185, 176–189. http://dx.doi.org/10.1016/j.energy.2019.07.055.

Chang, S., Castro-Lacouture, D., Yamagata, Y., 2020. Decision support for retrofitting building envelopes using multi-objective optimization under uncertainties. J. Build. Eng. 32, 101413. http://dx.doi.org/10.1016/j.jobe.2020.101413.

Chaturvedi, S., Rajasekar, E., Natarajan, S., 2020. Multi-objective building design optimization under operational uncertainties using the NSGA II algorithm. Buildings 10 (88), http://dx.doi.org/10.3390/buildings10050088.

Church, J., et al., 2013. Climate Change 2013: The Physical Science Basis. Contribution of Working Group I to the Fifth Assessment Report of the Intergovernmental Panel on Climate Change. Sea Level Change. pp. 1138–1191.

Costa-Carrapiço, I., Raslan, R., González, J.N., 2020. A systematic review of genetic algorithm-based multi-objective optimisation for building retrofitting strategies towards energy efficiency. Energy Build. 210, 109690. http://dx.doi.org/10.1016/j.enbuild.2019.109690.

D'Agostino, D., Parker, D., 2018. A framework for the cost-optimal design of nearly zero energy buildings (NZEBs) in representative climates across Europe. Energy 149, 814–829. http://dx.doi.org/10.1016/j.energy.2018.02.020.

D'Agostino, D., Parker, D., Epifani, I., Crawley, D., Lawrie, L., 2022. How will future climate impact the design and performance of nearly zero energy buildings (NZEBs)? Energy 240, 122479. http://dx.doi.org/10.1016/j.energy.2021.122479.

Deb, K., Pratap, A., Agarwal, S., Meyarivan, T., 2002. A fast and elitist multi-objective genetic algorithm: NSGA-II. IEEE Trans. Evol. Comput. 6, 182–197. http://dx.doi.org/10.1109/4235.996017.

Delgarm, N., Sajadi, B., Kowsary, F., Delgarm, S., 2016. Multi-objective optimization of the building energy performance: A simulation-based approach by means of particle swarm optimization (PSO). Appl. Energy 170, 293–303. http://dx.doi.org/10.1016/j.apenergy.2016.02.141.

https://energyplus.net/weather. Accessed 2022-05-01.

Evins, R., 2013. A review of computational optimisation methods applied to sustainable building design. Renew. Sustain. Energy Rev. 22, 230–245. http://dx.doi.org/10.1016/j.rser.2013.02.004.

García Kerdan, I., Raslan, R., Ruyssevelt, P., Morillón Gálvez, D., 2017. A comparison of an energy/economic-based against an exergoeconomic-based multi-objective optimisation for low carbon building energy design. Energy 128, 244–263. http://dx.doi.org/10.1016/j.energy.2017.03.142.

Ghaderian, M., Veysi, F., 2021. Multi-objective optimization of energy efficiency and thermal comfort in an existing office building using NSGA-II with fitness approximation: A case study. J. Build. Eng. 41, 102440. http://dx.doi.org/10.1016/j.jobe.2021.102440.

Gilani, S., O'Brien, W., 2021. Natural ventilation usability under climate change in Canada and the United States. Build. Res. Inf. 49, 367–386. http://dx.doi.org/10.1080/09613218.2020.1760775.

Grygierek, K., Ferdyn-Grygierek, J., 2018. Multi-objective optimization of the envelope of building with natural ventilation. Energies 11 (1383), http://dx.doi.org/10.3390/en11061383.

Guan, L., 2009. Preparation of future weather data to study the impact of climate change on buildings. Build. Environ. 44, 793–800. http://dx.doi.org/10.1016/j.buildenv.2008.05.021.

Güneralp, B., et al., 2017. Global scenarios of urban density and its impacts on building energy use through 2050. Proc. Natl. Acad. Sci. 114, 8945–8950. http://dx.doi.org/10.1073/pnas.1606035114.

Guo, R., Heiselberg, P., Hu, Y., Zhang, C., Vasilevskis, S., 2020. Optimization of night ventilation performance in office buildings in a cold climate. Energy Build. 225, 110319. http://dx.doi.org/10.1016/j.enbuild.2020.110319.

Guo, J.-X., Huang, C., 2020. Feasible roadmap for CCS retrofit of coal-based power plants to reduce Chinese carbon emissions by 2050. Appl. Energy 259, 114112. http://dx.doi.org/10.1016/j.apenergy.2019.114112.

Guo, S., Yan, D., Hu, S., Zhang, Y., 2021. Modelling building energy consumption in China under different future scenarios. Energy 214, 119063. http://dx.doi.org/10.1016/j.energy.2020.119063.

Harkouss, F., Fardoun, F., Biwole, P.H., 2018. Optimization approaches and climates investigations in NZEB—A review. Build. Simul. 11, 923–952. http://dx.doi.org/10.1007/s12273-018-0448-6.

He, Q., Hossain, M.U., Ng, S.T., Augenbroe, G., 2021. Identifying practical sustainable retrofit measures for existing high-rise residential buildings in various climate zones through an integrated energy-cost model. Renew. Sustain. Energy Rev. 151, 111578. http://dx.doi.org/10.1016/j.rser.2021.111578.

Hoegh-Guldberg, O., et al., 2019. The human imperative of stabilizing global climate change at 1.5oC. 365, eaaw6974. http://dx.doi.org/10.1126/science.aaw6974,

Hoyt, T., Arens, E., Zhang, H., 2015. Extending air temperature setpoints: Simulated energy savings and design considerations for new and retrofit buildings. Build. Environ. 88, 89–96. http://dx.doi.org/10.1016/j.buildenv.2014.09.010.

Hu, X., Xiang, Y., Zhang, H., Lin, Q., Wang, W., Wang, H., 2021. Active–passive combined energy-efficient retrofit of rural residence with non-benchmarked construction: A case study in Shandong province, China. Energy Rep. 7, 1360–1373. http://dx.doi.org/10.1016/j.egyr.2021.02.045.

Huang, L., Krigsvoll, G., Johansen, F., Liu, Y., Zhang, X., 2018. Carbon emission of global construction sector. Renew. Sustain. Energy Rev. 81, 1906–1916. http://dx.doi.org/10.1016/j.rser.2017.06.001.

IPCC, C.C., 2013. The Physical Science Basis. Contribution of Working Group I to the Fifth Assessment Report of the Intergovernmental Panel on Climate Change. Cambridge University Press, United Kingdom New York, NY, USA.

Jafarpur, P., Berardi, U., 2021. Effects of climate changes on building energy demand and thermal comfort in Canadian office buildings adopting different temperature setpoints. J. Build. Eng. 42, 102725. http://dx.doi.org/10.1016/j.jobe.2021.102725.

Jalilzadehazhari, E., Vadiee, A., Johansson, J., 2021. Subsidies required for installing renewable energy supply systems considering variations in future climate conditions. J. Build. Eng. 35, 101999. http://dx.doi.org/10.1016/j.jobe.2020.101999.

Javanroodi, K., Mahdavinejad, M., Nik, V.M., 2018. Impacts of urban morphology on reducing cooling load and increasing ventilation potential in hot-arid climate. Appl. Energy 231, 714–746. http://dx.doi.org/10.1016/j.apenergy.2018.09.116.

Jimenez-Bescos, C., 2017. An evaluation on the effect of night ventilation on thermal mass to reduce overheating in future climate scenarios. Energy Procedia 122, 1045–1050. http://dx.doi.org/10.1016/j.egypro.2017.07.476.

Karimpour, M., Belusko, M., Xing, K., Boland, J., Bruno, F., 2015. Impact of climate change on the design of energy efficient residential building envelopes. Energy Build. 87, 142–154. http://dx.doi.org/10.1016/j.enbuild.2014.10.064.

Klein, S.A., Duffie, J.A., Mitchell, J.C., Kummer, J.P., Thornton, J.W., Beckman, W.A., 2006. TRNSYS Transient Simulation Program. Solar Energy Laboratory, Univ. of Wisconsin-Madison, Madison, WI, USA.

Lapisa, R., Bozonnet, E., Salagnac, P., Abadie, M.O., 2018. Optimized design of low-rise commercial buildings under various climates – Energy performance and passive cooling strategies. Build. Environ. 132, 83–95. http://dx.doi.org/10.1016/j.buildenv.2018.01.029.

Li, M., Shi, J., Cao, J., Fang, X., Wang, M., Wang, X., 2020. Climate change impacts on extreme energy consumption of office buildings in different climate zones of China. Theor. Appl. Climatol. 140, 1291–1298. http://dx.doi.org/10.1007/s00704-020-03167-7.

Liu, B., Pouramini, S., 2021. Multi-objective optimization for thermal comfort enhancement and greenhouse gas emission reduction in residential buildings applying retrofitting measures by an Enhanced Water Strider Optimization Algorithm: A case study. Energy Rep. 7, 1915–1929. http://dx.doi.org/10.1016/j.egyr.2021.03.044.

Liu, J., Ren, J., Zhang, L., Xie, X., Kim, M.K., Zhang, L., 2019. Optimization of control strategies for the radiant floor cooling system combined with displacement ventilation: A case study of an office building in Jinan, China. Int. J. Archit. Eng. Technol. 6, 33–48. http://dx.doi.org/10.15377/2409-9821.2019.06.5.

Masui, T., et al., 2011. An emission pathway for stabilization at 6 Wm-2 radiative forcing. Clim. Change 109, 59. http://dx.doi.org/10.1007/s10584-011-0150-5.

Meng, F., Li, M., Cao, J., Li, J., Xiong, M., Feng, X., Ren, G., 2018. The effects of climate change on heating energy consumption of office buildings in different climate zones in China. Theor. Appl. Climatol. 133, 521–530. http://dx.doi.org/10.1007/s00704-017-2206-6.

MOHURD, 2021. General Specifications for Building Energy Conservation and Renewable Energy Utilization. China Architecture & Building Press.

Naji, S., Aye, L., Noguchi, M., 2021. Multi-objective optimisations of envelope components for a prefabricated house in six climate zones. Appl. Energy 282, 116012. http://dx.doi.org/10.1016/j.apenergy.2020.116012.

Nguyen, A.T., Rockwood, D., Doan, M.K., Dung Le, T.K., 2021. Performance assessment of contemporary energy-optimized office buildings under the impact of climate change. J. Build. Eng. 35, 102089. http://dx.doi.org/10.1016/j.jobe.2020.102089.

Nurlybekova, G., Memon, S.A., Adilkhanova, I., 2021. Quantitative evaluation of the thermal and energy performance of the PCM integrated building in the subtropical climate zone for current and future climate scenario. Energy 219, 119587. http://dx.doi.org/10.1016/j.energy.2020.119587.

Olonscheck, M., Holsten, A., Kropp, J.P., 2011. Heating and cooling energy demand and related emissions of the german residential building stock under climate change. Energy Policy 39, 4795–4806. http://dx.doi.org/10.1016/j.enpol.2011.06.041.

Oree, V., Khoodaruth, A., Teemul, H., 2016. A case study for the evaluation of realistic energy retrofit strategies for public office buildings in the Southern Hemisphere. Build. Simul. 9, 113–125. http://dx.doi.org/10.1007/s12273-015-0259-y.

Radhi, H., 2009. Evaluating the potential impact of global warming on the UAE residential buildings – A contribution to reduce the CO2 emissions. Build. Environ. 44, 2451–2462. http://dx.doi.org/10.1016/j.buildenv.2009.04.006.

Ren, J., Liu, J., Zhou, S., Kim, M.K., Miao, J., 2022. Developing a collaborative control strategy of a combined radiant floor cooling and ventilation system: A PMV-based model. J. Build. Eng. 54, 104648. http://dx.doi.org/10.1016/j.jobe.2022.104648.

Riahi, K., et al., 2011. RCP 8.5—A scenario of comparatively high greenhouse gas emissions. Clim. Change 109, 33. http://dx.doi.org/10.1007/s10584-011-0149-y.

Sarihi, S., Mehdizadeh Saradj, F., Faizi, M., 2021. A critical review of façade retrofit measures for minimizing heating and cooling demand in existing buildings. Sustain. Cities Soc. 64, 102525. http://dx.doi.org/10.1016/j.scs.2020.102525.

Shao, Y., Geyer, P., Lang, W., 2014. Integrating requirement analysis and multi-objective optimization for office building energy retrofit strategies. Energy Build. 82, 356–368. http://dx.doi.org/10.1016/j.enbuild.2014.07.030.

Shen, P., 2017. Impacts of climate change on U.S. building energy use by using downscaled hourly future weather data. Energy Build. 134, 61–70. http://dx.doi.org/10.1016/j.enbuild.2016.09.028.

Sobhani, H., Shahmoradi, F., Sajadi, B., 2020. Optimization of the renewable energy system for nearly zero energy buildings: A future-oriented approach. Energy Convers. Manage. 224, 113370. http://dx.doi.org/10.1016/j.enconman.2020.113370.

Solgi, E., Hamedani, Z., Fernando, R., Skates, H., Orji, N.E., 2018. A literature review of night ventilation strategies in buildings. Energy Build. 173, 337–352. http://dx.doi.org/10.1016/j.enbuild.2018.05.052.

Thomson, A.M., et al., 2011. RCP4.5: a pathway for stabilization of radiative forcing by 2100. Clim. Change 109, 77. http://dx.doi.org/10.1007/s10584-011-0151-4.

Tommerup, H., Svendsen, S., 2006. Energy savings in danish residential building stock. Energy Build. 38, 618–626. http://dx.doi.org/10.1016/j.enbuild.2005.08.017.

Tootkaboni, M.P., Ballarini, I., Corrado, V., 2021. Analysing the future energy performance of residential buildings in the most populated Italian climatic zone: A study of climate change impacts. Energy Rep. 7, 8548–8560. http://dx.doi.org/10.1016/j.egyr.2021.04.012.

van Vuuren, D.P., et al., 2011. RCP2.6: exploring the possibility to keep global mean temperature increase below 2 °C. Clim. Change 109, 95. http://dx.doi.org/10.1007/s10584-011-0152-3.

Vasaturo, R., van Hooff, T., Kalkman, I., Blocken, B., Van Wesemael, P., 2018. Impact of passive climate adaptation measures and building orientation on the energy demand of a detached lightweight semi-portable building. Build. Simul. 11, 1163–1177. http://dx.doi.org/10.1007/s12273-018-0470-8.

Verichev, K., Zamorano, M., Carpio, M., 2020. Effects of climate change on variations in climatic zones and heating energy consumption of residential buildings in the southern Chile. Energy Build. 215, 109874. http://dx.doi.org/10.1016/j.enbuild.2020.109874.

Vukadinović, A., Radosavljević, J., Đorđević, A., Protić, M., Petrović, N., 2021. Multi-objective optimization of energy performance for a detached residential building with a sunspace using the NSGA-II genetic algorithm. Sol. Energy 224, 1426–1444. http://dx.doi.org/10.1016/j.solener.2021.06.082.

Wan, K.K.W., Li, D.H.W., Lam, J.C., 2011. Assessment of climate change impact on building energy use and mitigation measures in subtropical climates. Energy 36, 1404–1414. http://dx.doi.org/10.1016/j.energy.2011.01.033.

Wan, K.K.W., Li, D.H.W., Pan, W., Lam, J.C., 2012. Impact of climate change on building energy use in different climate zones and mitigation and adaptation implications. Appl. Energy 97, 274–282. http://dx.doi.org/10.1016/j.apenergy.2011.11.048.

Wang, H., Chen, Q., 2014. Impact of climate change heating and cooling energy use in buildings in the United States. Energy Build. 82, 428–436. http://dx.doi.org/10.1016/j.enbuild.2014.07.034.

Wang, R., Lu, S., Feng, W., Xu, B., 2021a. Tradeoff between heating energy demand in winter and indoor overheating risk in summer constrained by building standards. Build. Simul. 14, 987–1003. http://dx.doi.org/10.1007/s12273-020-0719-x.

Wang, R., Lu, S., Zhai, X., Feng, W., 2021b. The energy performance and passive survivability of high thermal insulation buildings in future climate scenarios. Build. Simul. 15, 1209–1225. http://dx.doi.org/10.1007/s12273-021-0818-3.

Xie, Y., Hu, P., Zhu, N., Lei, F., Xing, L., Xu, L., 2020. Collaborative optimization of ground source heat pump-radiant ceiling air conditioning system based on response surface method and NSGA-II. Renew. Energy 147, 249–264. http://dx.doi.org/10.1016/j.renene.2019.08.109.

Xue, Q., Wang, Z., Chen, Q., 2022. Multi-objective optimization of building design for life cycle cost and CO2 emissions: A case study of a low-energy residential building in a severe cold climate. Build. Simul. 15, 83–98. http://dx.doi.org/10.1007/s12273-021-0796-5.

Zhai, Z.J., Helman, J.M., 2019. Implications of climate changes to building energy and design. Sustain. Cities Soc. 44, 511–519. http://dx.doi.org/10.1016/j.scs.2018.10.043.

Zhao, X., Huang, G., Lu, C., Zhou, X., Li, Y., 2020. Impacts of climate change on photovoltaic energy potential: A case study of China. Appl. Energy 280, 115888. http://dx.doi.org/10.1016/j.apenergy.2020.115888.

Zou, Y., Lou, S., Xia, D., Lun, I.Y.F., Yin, J., 2021a. Multi-objective building design optimization considering the effects of long-term climate change. J. Build. Eng. 44, 102904. http://dx.doi.org/10.1016/j.jobe.2021.102904.

Zou, Y., Xiang, K., Zhan, Q., Li, Z., 2021b. A simulation-based method to predict the life cycle energy performance of residential buildings in different climate zones of China. Build. Environ. 193, 107663. http://dx.doi.org/10.1016/j.buildenv.2021.107663.